Tikrit Journal of Engineering Sciences (2025); 32(1): 2335
DOI: http://doi.org/10.25130/tjes.32.1.19

IRAQI Academic Scientific Journals

ISSN: 1813-162X (Print); 2312-7589 (Online)

Tikrit Journal of Engineering Sciences

available online at: http://www.tj-es.com

TJES Tikrit Journal of Engineering Sciences

The Impact of Receiver Geometry with Nanofluid on the Performance of a Fresnel Collector

Manar S. M. Al-Jethelah *[a], Hussam S. Dheyab [a], Samer M. Khalaf [a], Khairul Habib [b], Kamaruzzaman Bin Sopian [b]

a Mechanical Engineering Department, College of Engineering, Tikrit University, Iraq.
b Universiti Teknologi PETRONAST, Seri Iskandar, Malaysia.

Keywords:
Fresnel reflector; Solar energy; Thermal performance; Nanofluid; Nusselt number.

Highlights:

- *Nano-alumina (NA) and nanocalcium carbonate (NC) were utilized in binary and ternary mixes of development self-compacting geopolymer concrete (SCGPC).*
- *Adding nanoparticles decreased the fresh properties of all SCGPC mixes.*
- *Mixes, including nano-alumina, were observed to be more cohesive and had better mechanical properties than mixes with NC.*
- *Incorporating NA and NC in binary and ternary mixes improved mechanical properties.*

ARTICLE INFO

Article history:

Received	09 Sep. 2024
Received in revised form	28 Sep. 2024
Accepted	05 Jan. 2025
Final Proofreading	17 Feb. 2025
Available online	24 Mar. 2025

Citation: Al-Jethelah MSM, Dheyab HS, Khalaf SM, Habib K, Sopian KB. **The Impact of Receiver Geometry with Nanofluid on the Performance of a Fresnel Collector**. *Tikrit Journal of Engineering Sciences* 2025; **32**(1): 2335.
http://doi.org/10.25130/tjes.32.1.19

Corresponding author:
Manar S. M. Al-Jethelah
Mechanical Engineering Department, College of Engineering, Tikrit University, Iraq.

Abstract: Solar energy devices have acquired growing attention to developing friendly-environment techniques. Linear Fresnel collector is preferred due to its low thermal losses. The present work numerically studied the impact of a linear Fresnel receiver geometry and utilizing TiO_2 on the performance of the collector. Circular and isosceles receivers were investigated. Three TiO_2 volume fractions were utilized: 0%, 2%, and 4%. The tested Reynolds number range was between 100 and 900. COMSOL Multiphysics 6.1, i.e., based on the Finite Element method, was used to solve the present problem. The circular receiver had significantly better comprehensive evaluation criteria than the triangular. The Nusselt number improved by 2.64% at Reynolds number 900 as 4% TiO_2 was added to the pure water. The triangular receiver friction factor was up to 16.7% lower than the circular for Reynolds number<300 and 4% TiO_2.

تأثير شكل انبوب ماص يجري بداخله مائع نانوني على أداء مجمع فرينل الشمسي

منار صالح مهدي[١]، حسام سامي ذياب[١]، سامر محمود خلف[١]، خيرل حبيب[٢]، قمر الزمان بن سوبيان[٢]

[١] قسم الهندسة الميكانيكية/ كلية الهندسة / جامعة تكريت / تكريت - العراق.

[٢] الجامعة التكنولوجية بتروناست/ سيري إسكندر- ماليزيا.

الخلاصة

الأجهزة الشمسية اكتسبت انتباه متنامي لتطوير تقنيات صديقة للبيئة. مجمعات فرنل الخطية مفضلة نظرا لقلة خسائرها الحرارية. الدراسة الحالية تناولت تأثير الشكل الهندسي لمستقبل فرنل الخطي واستعمال ثنائي أوكسيد التيتانيوم على أداء المجمع. تم دراسة مستقبلين دائري ومثلث متساوي الساقين. استعملت ثلاث نسب حجمية لثنائي أوكسيد التيتانيوم: ٠٪ و٢٪ و٤٪. مدى عدد رينولدز المدروس كان بين ١٠٠ و٩٠٠. تم استعمال برنامج (COMSOL Multiphysics 6.1) المعتمد على طريقة العناصر المحددة لحل المشكلة الحالية. المستقبل الاسطواني أظهر اداءً متميزًا مقارنة بالمثلث. تحسن عدد نسلت ٢,٦٤٪ عند عدد رينولدز ٩٠٠ وإضافة ٤٪ ثنائي أوكسيد التيتانيوم للماء النقي. معامل الاحتكاك للمستقبل انخفض ١٦,٧٪ مقارنة بالاسطواني لعدد رينولدز أقل من ٣٠٠ و٤٪ ثنائي أوكسيد التيتانيوم.

الكلمات الدالة: عاكس فرنل، طاقة شمسية، أداء حراري، مائع نانوني، عدد نسلت.

1.INTRODUCTION

Depleting the fossil fuels and their negative role in global warming forced governments to find other energy solutions. The most achievable solution for the energy issue is solar energy. Solar energy has many advantages, such as worldwide availability, clean energy, and being an unexpansive energy source [1]. Thermal solar energy storage costs less than photovoltaic panels [2]. Therefore, thermal solar collectors gained special attention. The common thermal solar collectors are flat plate, parabolic trough, compound trough, tower, dish, and Fresnel reflector [3, 4]. To upmost benefit of these collectors, researchers have worked to improve their thermal-hydraulic performance. The linear Fresnel collectors (Fig. 1) are low-cost, robust, and simple in design and manufacturing [5, 6]. The drawback of linear Fresnel collectors is their low efficiency compared to parabolic trough collectors [7, 8]. Therefore, the researchers have proposed and studied enhanced linear Fresnel collectors. Mokhtar et al. [9] numerically and experimentally studied heating water using a linear Fresnel collector with four circular absorber tubes, i.e., January and February. The thermal efficiency was higher than 29%, and the outlet temperature was around 347 K. Bellos et al. [10] numerically and experimentally investigated a linear Fresnel collector with a flat plate receiver. The proposed design produced a useful heat of up to 8.5 kW and 5.3 kW in summer and winter, respectively. The collector gained a thermal efficiency of up to 20% using the thermal oil as a working fluid. Cagnoli et al. [11] numerically studied 1-D, 2-D, and 3-D models of Fresnel circular bare and evacuated receivers. They found that the evacuated tube performance was below expectations and highly depended on the solar radiation. However, the wind impact was slight due to the evacuated receiver. Beltagy et al. [12] theoretically and experimentally analyzed the Fresnel collector with the circular tube. A secondary reflector was fixed facing the primary reflectors. A thermal daily efficiency of 40% was obtained. Qiu et al. [13] studied a linear Fresnel collector with eight circular receivers within a trapezoidal cavity. The proposed collector achieved 72.0% thermal efficiency. Lin et al. [14] theoretically and experimentally analyzed the performance of a linear Fresnel collector with ten circular tubes arranged in a V-shaped receiver. A 45% thermal efficiency was achieved. Yang et al. [15] numerically studied improving a linear Fresnel collector with circular receiver. The receiver was inserted with Kenics mixer, twisted tape, spaced Kenics mixer, and spaced twisted tape to improve the collector's performance. The Kenics mixer achieved the highest Nu and friction resistance coefficient, up to 298.8% and 5.6 times, respectively. Sheikholeslami and Ebrahimpour [16] numerically studied improving the linear Fresnel collector performance using nanofluid, i.e., Al_2O_3-water, and inserting a twisted tape in the collector circular receiver. The twisted tape enhanced Nu up to 7.138% and increased the friction factor to 20.019%. Adding nanofluid increased the thermal efficiency by 0.153%. Bellos et al. [17] enhanced a linear Fresnel collector by adding CuO nanoparticles to the working fluid, i.e., Syltherm 800, and fixing fins inside the circular receiver. The thermal efficiency improved by 0.82% for the finned receiver and 4% CuO. Montes et al. [18] proposed hybrid loops comprising a linear Fresnel receiver and studied its feasibility. The studied loops included evacuated and non-evacuated receivers. The authors found that the working temperatures highly impacted the non-evacuated receivers' performance. Haque et al. [19] reported that the most commonly investigated non-circular ducts were equilateral and square ducts with Al_2O_3 and CuO nanoparticles+ water. Bellos and Tzivanidis [20] numerically studied the performance of a Fresnel collector with a CuO-Sytherm 800 nanofluid as the working fluid. The authors found that the CuO-Sytherm 800 experienced a lower friction factor and a Nu enhancement of up to 5% than the thermal oil. Ghodbane et al. [21] assessed the performance of linear Fresnel solar collector with MWCNTs/DW nanofluids as a working fluid. The studied volume fractions

were 0.05%, 0.1%, and 0.3%. The volume fraction of 0.2% showed a 2.2 times improvement in PEC and a 2.7 times enhancement in the heat transfer coefficient. Salehi et al. [22] studied the impact of TiO2, Ni, Al, and Ag on the performance of linear Fresnel solar collector. The studied concentrations were from 0.01% to 2%. 2% vol. Adding Ag, Ni, TiO2, and Al improved the heat transfer coefficient by 11.6%, 10.6%, 5.7%, and 4.94%, respectively. Previous investigations studied linear Fresnel collectors with circular receivers. Also, utilizing nanofluid in linear Fresnel collectors has yet to be thoroughly studied in different receiver geometries. Furthermore, most studies investigated nano-Al_2O_3. Few studies investigated nano-TiO_2, although it showed improvement over Al_2O_3 at high Re numbers [20]. The present study numerically investigates the impact of the linear Fresnel collector receiver geometry and utilizing nano-TiO_2 at low Re numbers on the collector's thermal-hydraulic performance. Two receiver shapes were studied: circular and triangular. Also, three nanoparticles, i.e., TiO_2, volume fractions were studied: 0%, 2%, and 4%. It is worth mentioning that nanoparticles volume fractions are below 8% as high-volume fractions increase viscosity and consequently the pumping power [20]. To ensure laminar and fully developed flow inside the receiver, low Re numbers were studied, i.e., $100 \leq Re \leq 900$. The present work is organized as follows: Section 1 introduces the linear Fresnel collectors and reviews associated works, Section 2 describes the physical and mathematical models, Section 3 introduces the numerical model, i.e., governing equations, assumptions, boundary conditions, numerical solution, grid independency test, and validation, Section 4 displays the results and discusses them, and Section 5 concludes the investigation's main outcomes.

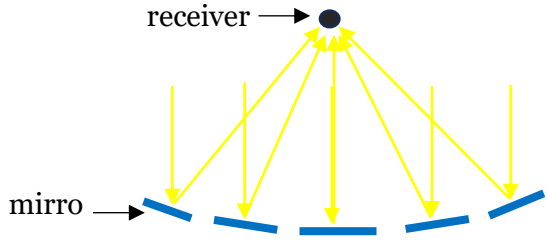

Fig. 1 Schematic of Linear Fresnel Collector.

2.PHYSICAL AND MATHEMATICAL MODELS

2.1.Physical Model

The present numerical analysis comprised two linear Fresnel receivers' shapes: circular and isosceles triangular, Fig. 2. Both receivers had the same fluid volume content to eliminate the fluid volume changes. Inside the receiver, the nanofluid flowed as a working fluid. The studied nanoparticles were for TiO_2, and the fluid was water. Table 1 tabulates the thermophysical properties of the studied materials.

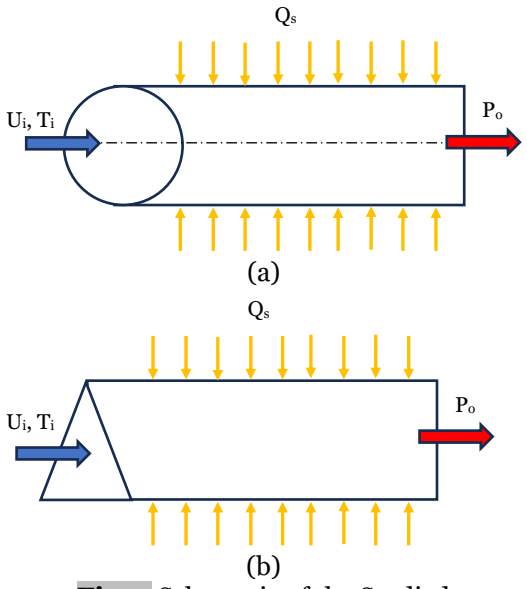

Fig. 2 Schematic of the Studied Configurations (a) Circular Receiver Tube (b) Isosceles Triangular Receiver Tube.

Table 1 Thermophysical Properties of Water and TiO_2 at 30 °C [23]

Material	Density (kg/m³)	Viscosity (Pa s)	Specific heat (J/kg K)	Thermal conductivity (W/m K)
Water	1000	8.94×10^{-4}	4184	0.613
TiO_2	4260	---	6890	11.70

2.2.Mathematical Model

The present analysis is based on the Reynolds number (Re), Nusselt number (Nu), friction factor (f), and comprehensive evaluation criteria (PEC).

The following equation expresses Re:

$$Re = \frac{\rho_f \, u \, D_h}{\mu_f} \quad (1)$$

The convection heat transfer coefficient can be calculated from:

$$h = \frac{Q_s}{T_s - T_m} \quad (2)$$

Nu is defined as:

$$Nu = \frac{h \, D_h}{k_f} \quad (3)$$

The friction factor is defined as [24]:

$$f = \frac{46}{Re} \quad (4)$$

The pressure drop can be calculated from:

$$\Delta P = \frac{f \, \rho \, u^2 \, L}{2 \, D_h} \quad (5)$$

Where the circular duct hydraulic diameters for is defined as:

$$D_h = \frac{4 \, A}{p} \quad (6)$$

The isosceles triangular duct hydraulic diameters can be defined as follows [25]:

$$D_h = \frac{B \sin\theta}{1+\sin\frac{\theta}{2}} \quad (7)$$

The comprehensive evaluation criteria (PEC) can be used to evaluate the receiver's performance. PEC can be expressed for nanoparticles impact as [25]

$$PEC = \frac{(Nu_{nf}/Nu_f)}{(f_{nf}/f_f)^{1/3}} \quad (8)$$

PEC for geometry impact can be expressed as

$$PEC = \frac{(Nu_{cir}/Nu_{tri})}{(f_{cir}/f_{tri})^{1/3}} \quad (9)$$

When PEC is above 1, adding nanoparticles to the working fluid positively impacts the heat transfer. On the other hand, PEC less than 1 reveals a negative impact by adding nanoparticles.

3.NUMERICAL MODEL

3.1.Governing Equations

Conservation of mass, momentum, and energy equations are used to describe the flow and temperature fields. Equations (10) to (12) represent the studied governing equations [26].

$$\nabla.(\rho_{nf}\vec{V}) = 0 \quad (10)$$

$$\nabla.(\rho_{nf}\vec{V}\,\vec{V}) = -\nabla P + \nabla.(\mu_{nf}\nabla\vec{V}) \quad (11)$$

$$\nabla.\left(\rho_{nf}\vec{V}\,c_{p_{nf}}\,T\right) = \nabla.(k_{nf}\nabla T) \quad (12)$$

The nanofluid density, viscosity, specific heat capacity, and thermal conductivity are defined as follows [27]:

$$\rho_{nf} = (1-\varphi)\rho_f + \varphi\rho_n \quad (13)$$

$$\mu_{nf} = [1 + 7.3\varphi + 123\varphi^2]\mu_f \quad (14)$$

$$c_{p_{nf}} = \frac{(1-\varphi)(\rho c_p)_f + \varphi(\rho c_p)_n}{\rho_{nf}} \quad (15)$$

$$k_{nf} = \left\{1 + 3\eta\varphi + \varphi^2\left[3\eta^2 + \frac{3\eta^3}{4} + \frac{9\eta^3}{16}\left(\frac{\frac{k_n}{k_f}+2}{2\frac{k_n}{k_f}+3}\right) + \frac{3\eta^4}{64} + \cdots\right]\right\}k_f \quad (16)$$

where $\eta = \frac{\frac{k_n}{k_f}-1}{\frac{k_n}{k_f}+2}$

3.2.Assumptions

The governing equations, Eqs. (7) to (9), are reduced from the general equations based on the following assumptions:

- The flow is steady, incompressible, and laminar.
- The nanofluid properties are temperature-independent.
- The nanoparticles and fluid are applied to the homogeneous single-phase model.
- The gravitational force, compression work, viscous dissipation, and receiver tube wall thermal resistance are neglected.

The simulation was terminated when the solution was converged as the residuals of the governing equations were equal or less than 10^{-5}.

3.3.Boundary Conditions

The governing equations, Eqs. (7) to (9), are solved under the boundary conditions defined below:

Inlet:	$u = U_i, v = w = 0, T = T_i$
Outlet:	$P = P_o, x\frac{\partial T}{\partial x} = 0$
Wall:	$u = v = w = 0, Q_s = -k_{nf}\frac{\partial T}{\partial n}\Big\|_s$
Symmetry plane:	$\frac{\partial u}{\partial y} = \frac{\partial u}{\partial z} = 0, v = 0, \frac{\partial T}{\partial y} = \frac{\partial T}{\partial z} = 0$

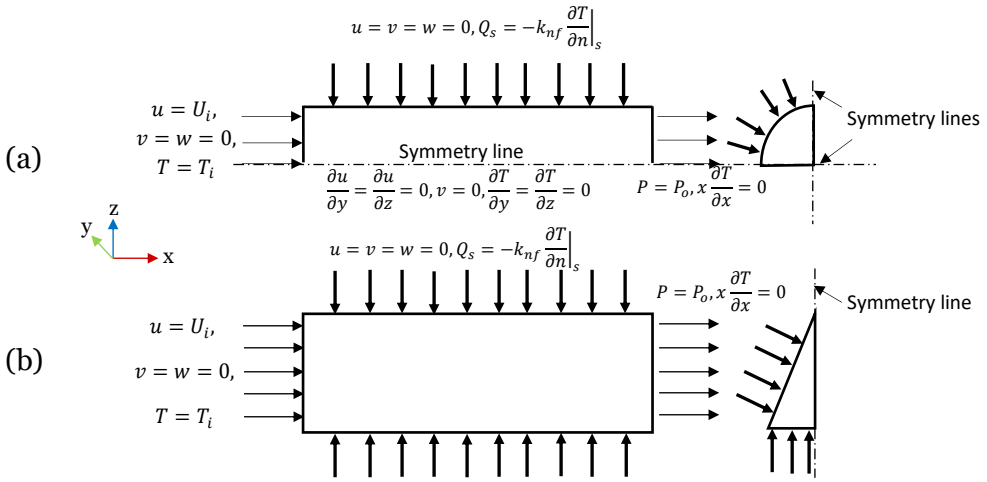

Fig. 3 Geometry, Boundary Conditions, and Coordinates of the Studied Problem for (a) Circular Receiver Tube (b) Isosceles Triangular Receiver Tube.

3.4.Numerical Solution

COMSOL Multiphysics was used to solve the present problem. The simulation flowchart is presented in Fig. (4). The finite element method was used through the Galerkin weighted residual method. The finite element solution commences partitioning the computational area into numerous simple shaped regions, i.e., elements, which could have different sizes and shapes depending on the geometry and the studied field. In each element, the interpolation functions are used to approximate the dependent variables. In the present work, an irregular grid shape and size were considered, especially adjacent to the receiver walls, to capture the dependent variables' rapid changes. The governing equations, i.e., Eqs. 10-12, are solved by transforming them into sets of algebraic equations, then solved using the iteration technique.

3.5.Grid Independency Test

The numerical solution includes using nodes to solve the governing equations under the specified boundary conditions and assumptions. To reduce/ eliminate the grid nodes' influence on the solution, a grid independence test must be performed. Besides grid indecency condition, the grid size is preferable to consume less time and computer calculations memory. The test was performed at Re= 500, heat flux of 500 W/m², and φ= 0%. Using Eq. (17), the finer mesh showed low mesh independency, i.e., less than 2%, for Nu and ΔP. Table 2 presents the grid independence test.

$$Error\% = \left|\frac{Nu_{extra\ fine} - Nu}{Nu_{extra\ fine}}\right| \%, \qquad (17)$$

$$Error\% = \left|\frac{\Delta P_{extra\ fine} - \Delta P}{\Delta P_{extra\ fine}}\right| \%$$

Figure 5 shows the mesh generated.

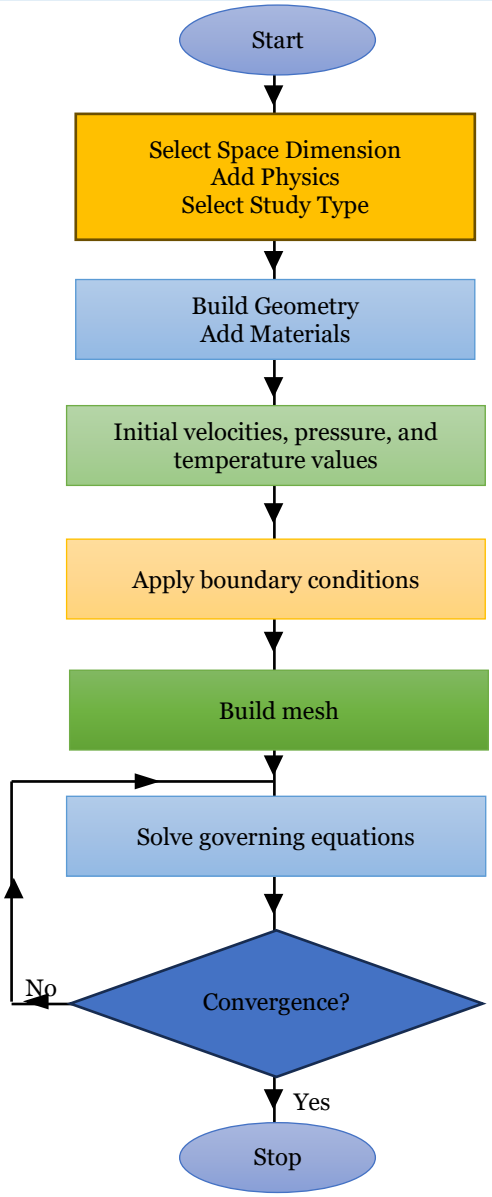

Fig. 4 Simulation Flowchart.

Table 2 Grid Independency Test.

No. of elements	Nu	Nu%	ΔP (Pa)	ΔP%
41433	14.437	-55.939	0.01651	-6.840
112944	12.376	-33.678	0.015676	-1.443
226336	11.271	-21.742	0.015453	0.000
644522	9.8859	-6.781	0.01537	0.537
1988928	9.4072	-1.610	0.01542	0.214
8392361	9.2581	---	0.015453	0.000

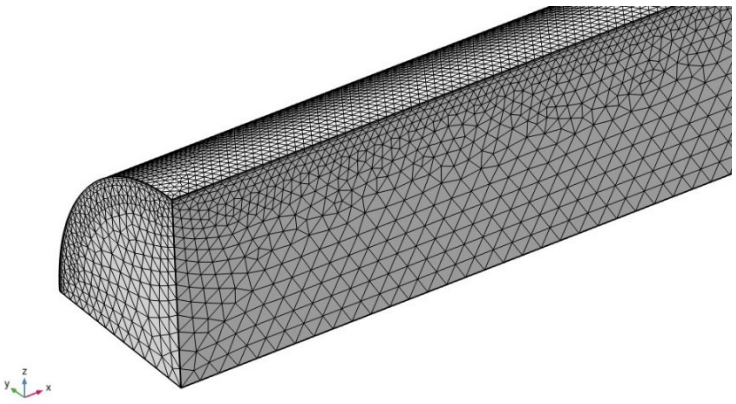

Fig. 5 The Mesh Generated.

3.6. Validation

To test the model accuracy, the present calculated Nu was compared with the Shah correlation (Eq. (18)) [28] and Sider-Date correlation (Eq. (19)) [15]. Also, the present calculated f was compared with the analytical one. A good agreement was achieved. Figures 6 to 8 show the validation results.

$$Nu_x = \begin{cases} 1.302\,X^{\frac{1}{3}} - 1, & X \le 0.00005 \\ 1.302\,X^{\frac{1}{3}} - 0.5, & 0.00005 < X < 0.001 \\ 4.364 + 8.68(10^3 X)^{-0.506}\,e^{-41X}, & X > 0.001 \end{cases} \quad (18)$$

$$N = 2.232\left(\frac{Re\,Pr_f}{L/D}\right)^{\frac{1}{3}}\left(\frac{\mu_f}{\mu_w}\right)^{0.14} \quad (19)$$

where $X = \frac{x/D}{Re\,Pr}$, and μ_f and μ_w are the fluid dynamic viscosity at the fluid mean and wall temperatures, respectively. The maximum deviation of the present results from the Shah correlation, Sider-Date correlation, and Eq. (4) were 7.45% (at Re=300), 9.26% (at Re=100), and 12.56% (at Re= 100), respectively, i.e., the last two percentages were extreme compared to other points.

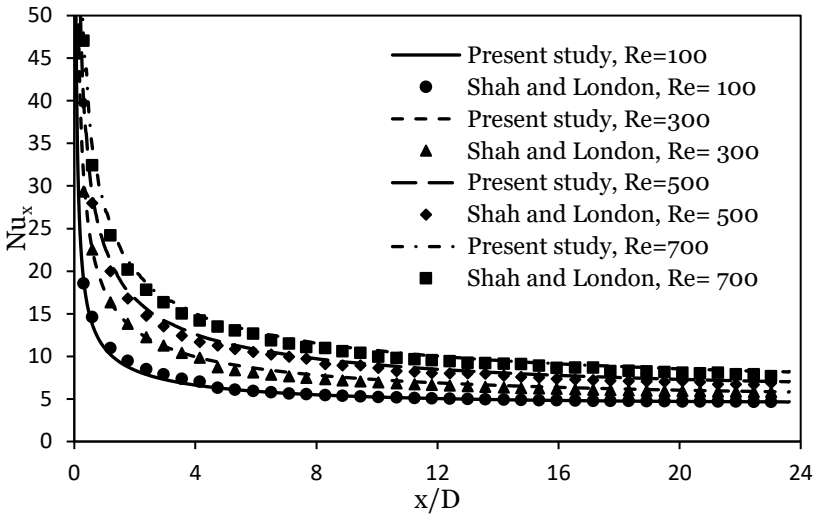

Fig. 6 Validation present results with Shah and London at Re=100, 300, and 500 [28].

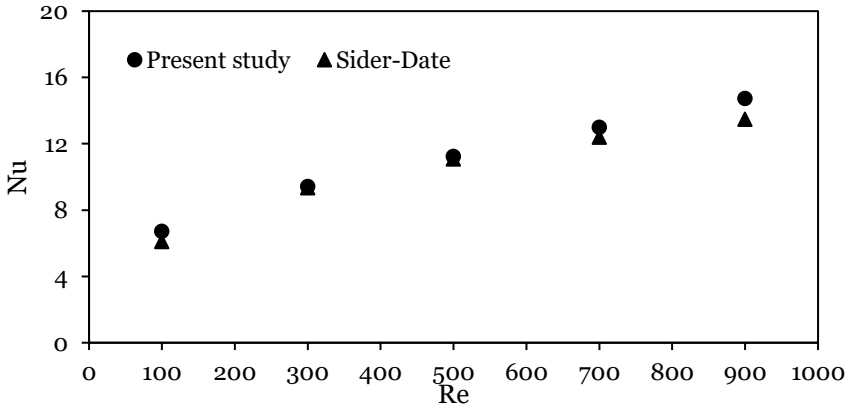

Fig. 7 Validation present results with Sider-Date [15].

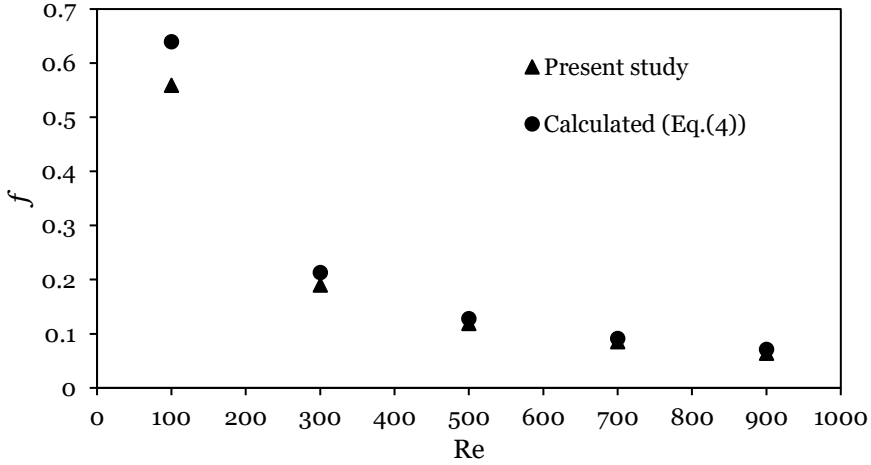

Fig. 8 Validation present results with calculated f (Eq. 4).

4.RESULTS AND DISCUSSION

The present study investigated the impact of linear Fresnel receive geometry and nanoparticles on the linear Fresnel collector performance. Circular and isosceles triangular receivers were studied. Tio_2 nanoparticles with volume fractions of 0%, 2%, and 4% were also studied. Figure 9 shows the impact of the receiver geometry on Nu for different Re and φ values. Increasing Re increased Nu. Higher Re means higher fluid velocity; as a result, fresh fluid replaces the warmed fluid faster. Therefore, the temperature difference between the fluid and the receiver wall increases, augmenting the heat transfer rate. The circular receiver showed better Nu than the isosceles for all studied Re and φ values. The circular Nu was 93.85%, 92.95%, and 93.09% higher than the isosceles triangular receiver at 0%, 2%, and 4%, respectively. Similar behavior was found by Salimpour and Dehshiri-Parizi [29] and Elfaghi et al. [26]. Figure 10 shows the impact of the receiver geometry on *f* for different Re and φ values. The friction factor decreases with increasing Re due to the increase in the inertia effect and the decrease in the viscous effect. The isosceles triangular receiver friction factor was lower than the circular because less fluid exposed to the duct wall. The friction factor sharply declined with increasing Re to 300. Then, the friction factor decline was less. At φ= 0%, the isosceles triangular receiver friction factor before Re=300 was 16% less than the circular. Then, the difference between the two geometries decreased to 9.63%. For φ= 2%, the same difference percentages and 4% were 16.47% and 10.16%; for φ= 4%, the differences were 16.60% and 10.8%. Figure 11 shows the nano-TiO_2 impact on Nu for different Re numbers ($100 \leq Re \leq 900$). The nano-TiO_2 impact was insignificant for the studied volume fractions due to the low nano-TiO_2 thermal conductivity and high specific capacity. For the circular receiver, adding 2% nano-TiO_2 improved Nu by 1.71% at Re=900. Nu improved by 2.64% by adding 4% nano-TiO_2. For the isosceles triangular receiver, Nu improved by 1.50% and 2.27% by adding 2% and 4%, respectively, at Re= 300. Increasing Nu with adding the nanoparticles is due to improving the nanofluid's thermal conductivity, enhancing the heat transfer coefficient, compared to the pure fluid. Figure 12 shows the nano-TiO_2 impact on the friction factor *f* for different Re numbers. Adding nanoparticles to a fluid increases its viscosity; as a result, adding nanoparticles increases the friction factor. The friction factor in the circular receiver increased by 12.03% by adding 2% nano-TiO_3 and 31.28% by adding 4%. As for the triangular receiver, the friction factor increments were 11.89% by adding 2% nano-TiO2 and 30.91% by adding 4% nano-TiO_2. Comparing Figs. 10 and 11 implies that adding nano-TiO_2 slightly improved Nu while significantly increased the friction factor for both studied geometries. The same trend was detected by Khashaei et al. [30].

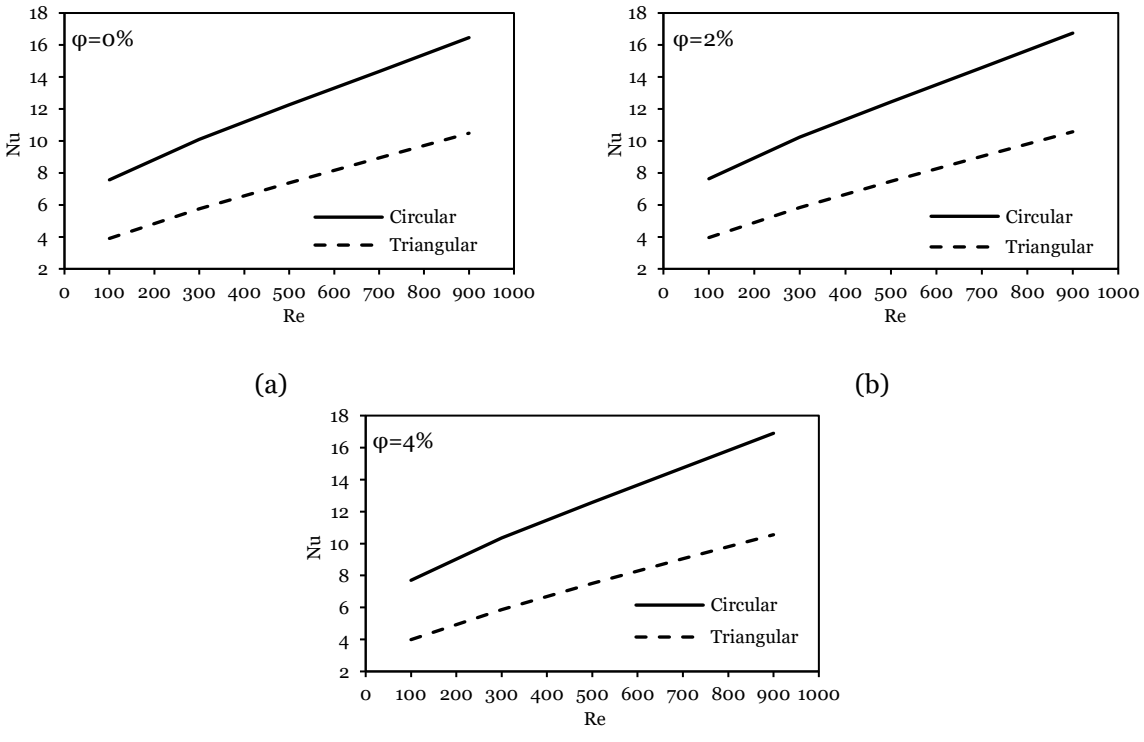

Fig. 9 Impact of Receiver Geometry on Nu at φ= (a) 0%, (b) 2%, and (c) 4%.

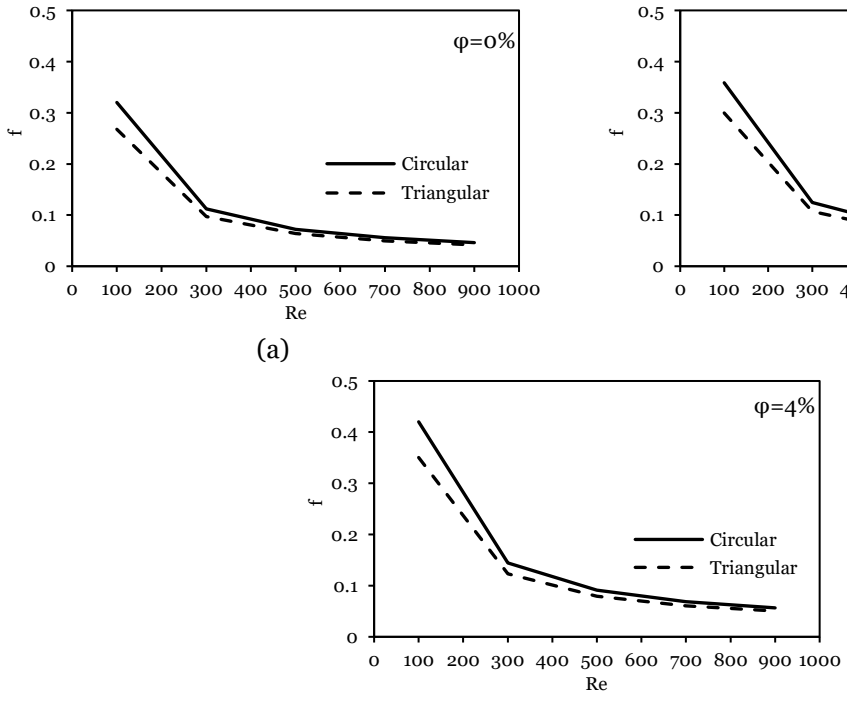

Fig. 10 Impact of receiver geometry on *f* at φ= (a) 0%, (b) 2%, and (c) 4%.

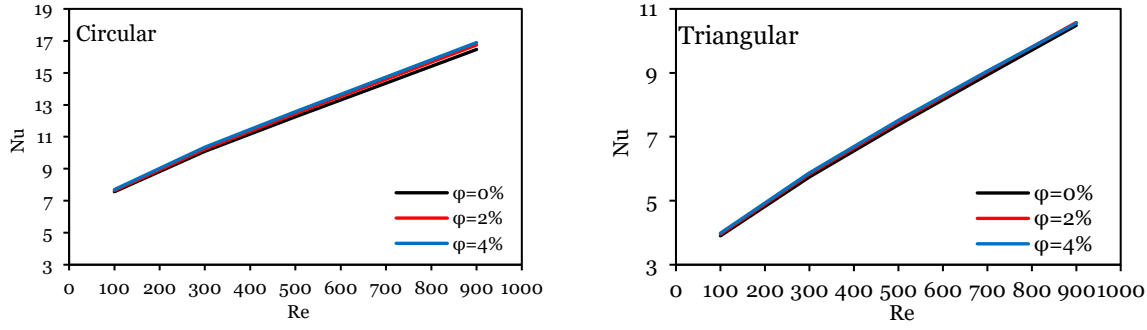

Fig. 11 Impact of nano-TiO_2 on Nu in (a) circular and (b) triangular receivers.

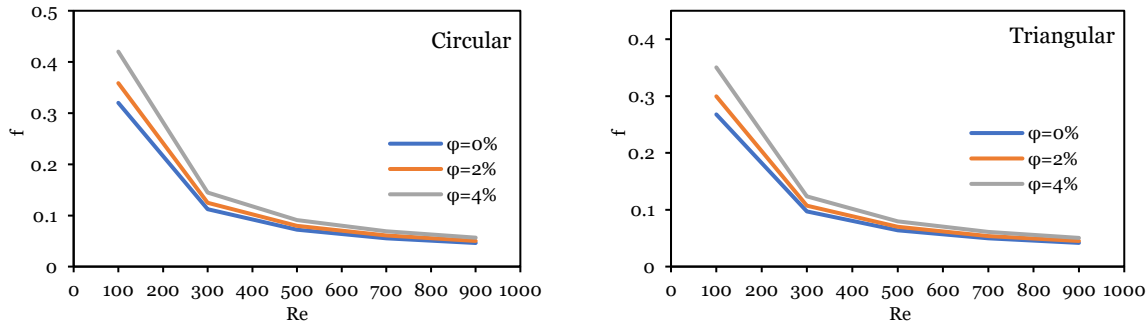

Fig. 12 Impact of nano-TiO_2 on *f* in (a) circular and (b) Triangular receivers.

Figure 13 shows the impact of adding nano-TiO_2 on PEC versus Re. PEC increased with Re due to the increase in nano-TiO2 bulk motion and the shear stress due to the increase in the velocity gradient caused by increasing Re. The difference between the circular and isosceles triangular was insignificant for both studied volume fractions. The improvement in Nu due to adding nano-TiO_2 was lower than the increase in the friction factor. As a result, PEC was lower than 1, implying that nano-TiO2 negatively impacted the receiver's overall thermal-hydraulically performance. Figure 14 depicts the impact of the receiver geometry on the PEC for different TiO_2 volume fractions, i.e., 0%, 2%, and 4%. The geometry PEC was above 1 using pure water. While, the geometry PEC, for both studied nano-TiO_2 volume fractions, was below 1. This result reveals that TiO_2 hindered the thermal-hydraulic enhancement.

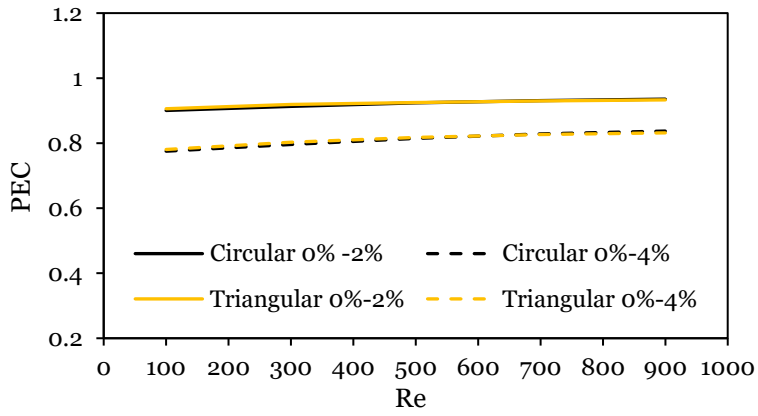

Fig. 13 PEC Versus Re for Circular and Isosceles Triangular Receivers.

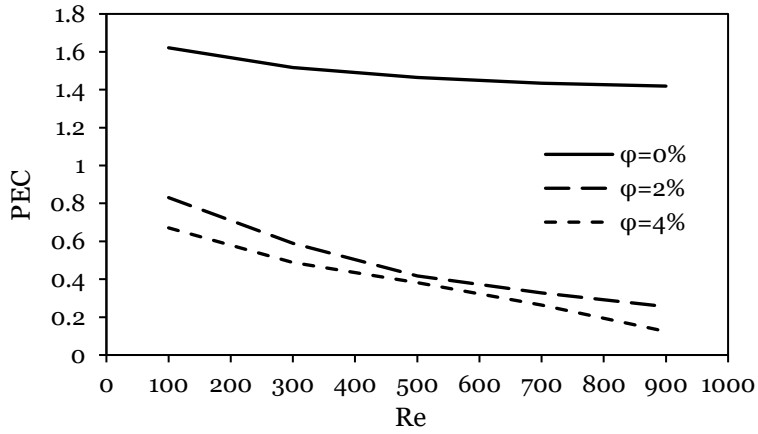

Fig. 14 PEC versus Re at φ= (a) 0%, (b) 2%, and (c) 4%.

5.CONCLUSIONS

The present study numerically investigated the impact of the linear Fresnel receiver geometry and nanofluid on the receiver's performance. Two geometries were studied, i.e., circular and isosceles triangular ducts. TiO_2-water was utilized as a nanofluid. The study included a Re numbers range of $100 \leq Re \leq 900$. The key concluded points are:

- Nu in the circular receiver was higher than the triangular by 93.85% with 0% TiO_2.
- The friction factor in the triangular receiver was lower than that in the circular receiver, up to 16.47% at 4% TiO_2 and Re below 300.
- Compared to pure water, adding 4% TiO_2 improved Nu by 2.64% at Re=900 for the circular receiver and 2.27% for the triangular.
- Adding 4% nano-TiO_2 increased the friction factor by 31.28% for the circular receiver and 30.91% for the triangular.
- PEC was below one for adding 2% and 4% TiO_2 for both studied geometries.
- The circular receiver showed better PEC than the triangular, especially in the pure case.
- As a future work, the Fresnel collector can be integrated with thermal storage, and the collector performance can be studied for an extended time after sunset.

REFERENCES

[1] Dheyab HS, Al-Jethelah M, Ibrahim TK, Sirine Chtourou, Mounir Baccar. **Closed Solar Air Heater System Integrated with PCM (RT42 and RT50) in a Thermal Storage-Finned Heat Exchanger Unit.** *Tikrit Journal of Engineering Sciences* 2023;**30**(3):27-37.

[2] Kennedy KM, Ruggles TH, Rinaldi K, Dowling JA, Duan L, Caldeira K, et al. **The Role of Concentrated Solar Power with Thermal Energy Storage in Least-Cost Highly Reliable Electricity Systems Fully Powered by Variable Renewable Energy.** *Advances in Applied Energy* 2022; **6**:100091.

[3] Ko GK, Gomna A, Falcoz Q, Coulibaly Y, Olives R. **A Review of Linear Fresnel Collector Receivers Used in Solar Thermal Technology.** *Physical Science International Journal* 2022; **26**(8):21-40.

[4] Farhan IS, Mohammed AA, Al-Jethelah MSM. **The Effect of Uneven Metal Foam Distribution on Solar Compound Parabolic Trough Collector Receiver Thermal Performance.** *Tikrit Journal of Engineering Sciences* 2024; **31**(1):291-305.

[5] Montes MJ, Rubbia C, Abbas R, Martínez-Val JM. **A Comparative Analysis of Configurations of Linear Fresnel Collectors for Concentrating Solar Power.** *Energy* 2014; **73**:192-203.

[6] Platzer WJ, Mills D, Gardner W. **Linear Fresnel Collector (LFC) Solar Thermal Technology.** *Concentrating Solar Power Technology*. 2021. Elsevier. p. 165-217.

[7] Morin G, Dersch J, Platzer W, Eck M, Häberle A. **Comparison of Linear Fresnel and Parabolic Trough Collector Power Plants.** *Solar Energy* 2012; **86**(1):1-12.

[8] Schenk H, Hirsch T, Fabian Feldhoff J, Wittmann M. **Energetic Comparison of Linear Fresnel and Parabolic Trough Collector Systems.** *Journal of Solar Energy Engineering* 2014; **136**(4): 041015.

[9] Mokhtar G, Boussad B, Noureddine S. **A Linear Fresnel Reflector as a Solar System for Heating Water: Theoretical and Experimental Study.** *Case Studies in Thermal Engineering* 2016; **8**:176-186.

[10] Bellos E, Mathioulakis E, Tzivanidis C, Belessiotis V, Antonopoulos KA. **Experimental and Numerical Investigation of a Linear Fresnel Solar Collector with Flat Plate Receiver.** *Energy Conversion and Management* 2016; **130**:44-59.

[11] Cagnoli M, Mazzei D, Procopio M, Russo V, Savoldi L, Zanino R. **Analysis of the Performance of Linear Fresnel Collectors: Encapsulated vs. Evacuated Tubes.** *Solar Energy* 2018; **164**:119-138.

[12] Beltagy H, Semmar D, Lehaut C, Said N. **Theoretical and Experimental Performance Analysis of a Fresnel Type Solar Concentrator.** *Renewable Energy* 2017; **101**:782-793.

[13] Qiu Y, He Y-L, Wu M, Zheng Z-J. **A Comprehensive Model for Optical and Thermal Characterization of a Linear Fresnel Solar Reflector with a Trapezoidal Cavity Receiver.** *Renewable Energy* 2016; **97**: 129-144.

[14] Lin M, Sumathy K, Dai YJ, Wang RZ, Chen Y. **Experimental and Theoretical Analysis on a Linear Fresnel Reflector Solar Collector Prototype With V-Shaped Cavity Receiver.** *Applied Thermal Engineering* 2013;**51**(1-2):963-972.

[15] Yang N, Liu Q, Xuan J, Wang B, Xing L. **Enhancing Optical and Thermohydraulic Performance of Linear Fresnel Collectors with Receiver Tube Enhancers: A Numerical Study.** *International Journal of Heat and Mass Transfer* 2024; **231**:125850.

[16] Sheikholeslami M, Ebrahimpour Z. **Thermal Improvement of Linear Fresnel Solar System Utilizing Al2O3-Water Nanofluid and Multi-Way Twisted Tape.** *International Journal of Thermal Sciences* 2022; **176**:107505.

[17] Bellos E, Tzivanidis C, Papadopoulos A. **Enhancing the Performance of a Linear Fresnel Reflector Using Nanofluids and Internal Finned Absorber.** *Journal of Thermal Analysis and Calorimetry* 2019; **135**(1):237-255.

[18] Montes MJ, Abbas R, Muñoz M, Muñoz-Antón J, Martínez-Val JM. **Advances in the Linear Fresnel Single-Tube Receivers: Hybrid Loops with Non-Evacuated and Evacuated Receivers.** *Energy Conversion and Management* 2017; **149**:318-333.

[19] Haque ME, Hossain MS, Ali HM. **Laminar Forced Convection Heat Transfer of Nanofluids Inside Non-Circular Ducts: A Review.** *Powder Technology* 2021; **378**: 808-830.

[20] Bellos E, Tzivanidis C. **Multi-Criteria Evaluation of a Nanofluid-Based Linear Fresnel Solar Collector.** *Solar Energy* 2022; **163**:200-214.

[21] Ghodbane M, Said Z, Hachicha AA, Boumeddane B. **Performance Assessment of Linear Fresnel Solar Reflector Using MWCNTs/DW Nanofluids.** *Renewable Energy* 2020; **151**:43-56.

[22] Salehi N, Mirabdolah Lavasani A, Mehdipour R, Eftekhari Yazdi M. **Effect of Nano Fluids on the Thermal Performance and Efficiency of Linear Fresnel Collector in Hot Summer Months.** *Journal of Renewable Energy and Environment* 2021;(Online First).

[23] Devireddy S, Mekala CSR, Veeredhi VR. **Improving the Cooling Performance of Automobile Radiator with Ethylene Glycol Water Based TiO2 Nanofluids.** *International Communications in Heat and Mass Transfer* 2016; **78**:121-126.

[24] Syam Sundar L, Alklaibi AM, Sambasivam S, Chandra Mouli KVV. **Experimentally Determining the Thermophysical Properties, Heat Transfer and Friction Factor Fe3O4-TiO2 Magnetic Hybrid Nanofluids in a Mini-Heat Sink Under Magnetic Field: Proposing New**

Correlations. *Journal of Magnetism and Magnetic Materials* 2024; **594**: 171889.

[25] Uddin N. **Fluid Mechanics - A Problem-Solving Approach.** 1st ed. UK: Taylor and Francis Group; 2023.

[26] Elfaghi AM, Abosbaia AA, Alkbir MF, Omran AA. **CFD Simulation of Forced Convection Heat Transfer Enhancement in Pipe Using Al2O3/Water Nanofluid.** *Journal of Advanced Research in Micro and Nano Engineering* 2022; **7**(1):8-13.

[27] Al-Sammarraie AT, Al-Jethelah M, Salimpour MR, Vafai K. **Nanofluids Transport Through a Novel Concave/Convex Convergent Pipe.** *Numerical Heat Transfer, Part A: Applications* 2019; **75**(2):91-109.

[28] Jahanbin A. **Comparative Study on Convection and Wall Characteristics of Al2O3-Water Nanofluid Flow Inside a Miniature Tube.** *Engineering Journal* 2016; **20**(3):169-181.

[29] Salimpour MR, Dehshiri-Parizi A. **Convective Heat Transfer of Nanofluid Flow Through Conduits with Different Cross-Sectional Shapes.** *Journal of Mechanical Science and Technology* 2015; **29**(2):707-713.

[30] Khashaei A, Ameri M, Azizifar S. **Heat Transfer Enhancement and Pressure Drop Performance of Al2O3 Nanofluid in a Laminar Flow Tube with Deep Dimples Under Constant Heat Flux: An Experimental Approach.** *International Journal of Thermofluids* 2024; **24**:100827.